

A Kernel-based Signal Localization Method for NIRS Brain-computer Interfaces

Zhang Haihong, Guan Cuntai
Institute for Infocomm Research
21 Heng Mui Keng Terrace, Singapore
{hhzhang,ctguan}@i2r.a-star.edu.sg

Abstract

This paper presents a novel method for signal localization for building high-performance brain-computer interfaces using Near-Infrared Spectroscopy. It first proposes a kernel-based model to represent haemodynamic signals of interest under parameterized transformations. A mathematical solution is therefore derived to locate the signals by estimating the parameters. We employ a support vector machine to classify the located signals into left/right hand movements. We evaluate the method on both simulated and real world data, with positive results suggesting the method's high efficacy. This work can be extended to other systems using e.g. fMRI and EEG.

1. Introduction

Brain-computer interface (BCI) is an emerging technology which aims to convey people's intentions to the outside world directly from their thoughts [1]. It is especially appealing to severely paralyzed patients, since motor ability is no longer a prerequisite for this communication.

In the past, a number of non-invasive BCI systems have been demonstrated (e.g. [2, 3]), mostly using surface electroencephalogram (EEG). However, it is well-known that surface EEG has limited anatomical specificity when compared with other functional brain imaging techniques.

Recently, an optical method called near-infrared spectroscopy (NIRS) has emerged as an alternative and direct way of brain functional imaging through the intact skull. In this method, the optical response of near-infrared rays is associated with regional brain activations in terms of e.g. oxygenated hemoglobin (Oxy-HB) or deoxygenated hemoglobin (deoxy-HB). As stated in [4], NIRS has a few merits like high degree of flexibility, high biochemical specificity and high sensitivity in detecting small substance concentrations. It is suggested [5, 6] that NIRS is promising for next-generation BCI systems by characterizing the haemodynamic responses to imaginary movements.

The study on NIRS signals for BCI, however, is still in its infancy. In particular, the variations among the haemodynamic signals in response to specific motor imaginations have yet to be addressed well in previous works. It is a critical problem since the variations will naturally occur due to the inevitable inconsistency in the execution of motor imaginations. For example, a subject may actually start an imagination at different start point and tempo in different mental state in each trial, bringing considerable difficulties to the recognition of the haemodynamic signals.

This work is our first attempt to address the variations among the NIRS haemodynamic signals for BCI. The objective here is to locate the haemodynamic signals in response to motor imaginations that are subject to a few types of variations. To this end, we first propose a kernel-based representation model in a statistical framework for the signals under parameterized variations. Furthermore, a mathematical solution is derived to locate the signals. Finally, we use support vector machines on located signals to differentiate imaginary movements.

We have conducted both computer simulation and real experimental study to examine the proposed method. The simulation uses computer-generated data to evaluate the robustness of the localization method against additive noises. The experimental study involves five healthy subjects performing real motor imaginations. The results suggest that the proposed method is effective in dealing with the variations, giving rise to a BCI system with significantly enhanced performance.

2. Problem Formulation

Let's first consider a multi-dimensional NIRS signal $y(t)$, obtained with sensors above the motor cortex region. In our NIRS-BCI setting, the signal is acquired in a protocol as illustrated in Fig. 1. Each trial will start with a beep sound; at 2 seconds, the subject will be asked to perform imaginations of left/right hand movements for 10 seconds; the last 8-second time is for the subject to rest.

Many factors may affect the execution of an imagination,

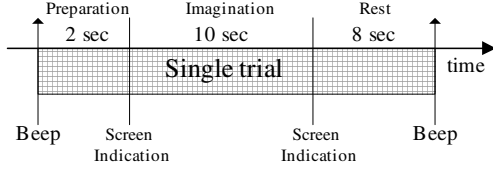


Figure 1. Single Trial Timing

yielding variable NIRS signals. Here we consider three major factors. Firstly, the subject may perform imaginations at different speed, resulting in tempo changes in the NIRS signals. Secondly, actual imaginations may start at different time point in each trial. Finally, varying mental state will cause changes in base level of the signals.

Now we define a mathematical model to describe these variation factors. Assume there is a model signal $\mathbf{y}_m(t)$, and each observed signal $\mathbf{y}(t)$ is a transformed instance. The first factor above implies a time shift (t); the second implies a change of tempo factor (a); and the last one would lead to difference (c) in the signal's base level. In other words, each instance takes a form of $\mathbf{y}_m(at+b)+c$. Hence, the localization of the signal turns out to be a searching problem whose objective is to find particular $\{a, b, c\}$ by

$$\operatorname{argmin}_{\{a,b,c\}} \{ \|\mathbf{y}(t) - (\mathbf{y}_m(at+b)+c)\|^2 \} \quad (1)$$

We will derive a mathematical solution to the problem in the following sections.

3. The Localization Method

3.1 The Kernel-based Signal Model

Given a signal consisting of a few samples at a sequence of time-point, e.g. $\Omega : \{\mathbf{y}_i, t_i\} i = 1 \cdots N$, we use the density function $f(\mathbf{y}, t)$ as a representation of the signal since it precisely characterizes the joint probability distribution of the samples. Real NIRS signals usually have shear complexity that makes it hard to describe the density functions with generic parametric methods. Thus, a non-parametric method called kernel density estimate is favored [7] here:

$$f(\mathbf{y}, t) = \frac{\alpha}{N} \sum_{i=1}^N k_y(\|\mathbf{y} - \mathbf{y}_i\|^2) k_t(\|t - t_i\|^2) \quad (2)$$

where k is the kernel function and takes a Gaussian form in this paper.

Therefore, the similarity between two signals, say Ω_p and Ω_q , can be defined by

$$D_0(p, q) = - \int \|f_p - f_q\|^2 dy dt \quad (3)$$

It follows mathematical manipulations that

$$\begin{aligned} D_0(p, q) = & \\ & - \frac{1}{N_p^2} \sum_{i,j} k_y\left(\frac{\|\mathbf{y}_i^{(p)} - \mathbf{y}_j^{(p)}\|^2}{2}\right) k_t\left(\frac{\|t_i^{(p)} - t_j^{(p)}\|^2}{2}\right) \\ & + \frac{2}{N_p N_q} k_y\left(\frac{\|\mathbf{y}_i^{(p)} - \mathbf{y}_j^{(q)}\|^2}{2}\right) k_t\left(\frac{\|t_i^{(p)} - t_j^{(q)}\|^2}{2}\right) \\ & - \frac{1}{N_q^2} \sum_{i,j} k_y\left(\frac{\|\mathbf{y}_i^{(q)} - \mathbf{y}_j^{(q)}\|^2}{2}\right) k_t\left(\frac{\|t_i^{(q)} - t_j^{(q)}\|^2}{2}\right) \end{aligned} \quad (4)$$

Now let's take into account the variation factors (see Section 2). For clarity, henceforth we note the model signal with Ω_p and its transformed instance with Ω_q . The Ω_p undergoes the transformation T will have

$$(\hat{t})_i = T(t)_i = at_i + b \quad \text{and} \quad \mathbf{y}(\hat{t}) = \mathbf{y}(t) + c \quad (5)$$

To reduce the complexity, we tentatively remove the DC components from both $\mathbf{y}(\hat{t})$ and $\mathbf{y}(t)$ and thus the factor c can be cancelled. Note that in subsection 3.3 we will show how to handle c in the final program.

Furthermore, by substituting t_i with \hat{t}_i in Eq. 4 and after some manipulations we have the similarity between two signals with respect to transformation T :

$$\begin{aligned} D_0(p_T, q) = & \\ & - \frac{1}{N_p^2} \sum_{i,j} k_y\left(\frac{\|\mathbf{y}_i^{(p)} - \mathbf{y}_j^{(p)}\|^2}{2}\right) k_t\left(\frac{a^2\|t_i^{(p)} - t_j^{(p)}\|^2}{2}\right) \\ & + \frac{2}{N_p N_q} k_y\left(\frac{\|\mathbf{y}_i^{(p)} - \mathbf{y}_j^{(q)}\|^2}{2}\right) k_t\left(\frac{\|at_i^{(p)} + b - t_j^{(q)}\|^2}{2}\right) \\ & - \frac{1}{N_q^2} \sum_{i,j} k_y\left(\frac{\|\mathbf{y}_i^{(q)} - \mathbf{y}_j^{(q)}\|^2}{2}\right) k_t\left(\frac{\|t_i^{(q)} - t_j^{(q)}\|^2}{2}\right) \\ & \triangleq -I_1 + I_2 - I_3 \end{aligned} \quad (6)$$

Since the term I_3 is not a function on $\{a, b\}$, we exclude them from the expression and define $D(p_T, q) = -I_1 + I_2$.

The formulated localization problem (Section 2) thus turns out to be an optimization problem: to search for the parameter T which yields the maximal similarity $D(p_T, q)$. Thanks to the smoothness of the Gaussian kernel based similarity measure, the maximal point will be reached at

$$\nabla D(p_T, q) = \frac{\partial D}{\partial a} \Delta a + \frac{\partial D}{\partial b} \Delta b = 0 \quad (7)$$

which implies $\frac{\partial D}{\partial a} = 0$ and $\frac{\partial D}{\partial b} = 0$. In the next sections we will derive a mathematical solution to Eq. 7.

3.2. The Iterative Equations

As in (Eq. 6) I_1 in $D()$ is independent of b , we have

$$\nabla_b D(p_T, q) = \nabla_b I_2 = \sum_{i,j} w_{ij} (at_i^{(p)} + b - t_j^{(q)}) \quad (8)$$

where

$$w_{ij} = \frac{2}{N_p N_q} k_y \left(\frac{\|y_i^{(p)} - y_j^{(q)}\|^2}{2} \right) g_t \left(\frac{\|at_i^{(p)} + b - t_j^{(q)}\|^2}{2} \right) \quad (9)$$

And g_t here is the derivative function of k_t . Set $D(p_T, q) = 0$ and we have the update function for b :

$$b = \frac{\sum_{i,j} -w_{ij}(at_i^{(p)} - t_j^{(q)})}{\sum_{i,j} w_{ij}} \quad (10)$$

which is actually an iterative function for b which is present on both sides (note w_{ij} is a function of b).

Let's now consider $\nabla_a D(p_T, q)$. For I_1 and I_2 there is

$$\nabla_a I_1(p_T, q) = \sum_{i,j} \beta_{i,j} a \quad (11)$$

$$\nabla_a I_2(p_T, q) = \sum_{i,j} w_{ij} t_i^{(p)} (at_i^{(p)} + b - t_j^{(q)})$$

where $\beta_{i,j} = \frac{\|t_i^{(p)} - t_j^{(q)}\|^2}{N_p^2} k_y \left(\frac{\|y_i^{(p)} - y_j^{(q)}\|^2}{2} \right) g_t \left(\frac{a^2 \|t_i^{(p)} - t_j^{(q)}\|^2}{2} \right)$.

Set $\nabla_a (-I_1 + I_2) = 0$ and we have

$$a = \frac{\sum_{i,j} w_{ij} t_i^{(p)} (b - t_j^{(q)})}{\sum_{i,j} \beta_{i,j} - \sum_{i,j} w_{ij} (t_i^{(p)})^2} \quad (12)$$

3.3. The Iterative Localization Algorithm

In real NIRS-BCI situations, we will be given a trial signal Ω_{q0} , which normally includes not only the transformed model signal Ω_q but also some irrelevant signals in the actual pre-motor-imagery and post-motor-imagery time periods. Thus the desired observation Ω_q may not be available directly. We address this problem with a practical algorithm shown below using the above mathematical solution.

1. Initialize the estimations of a and b .
2. Do the following steps.
3. With estimated a, b , extract from Ω_{q0} the hypothesized signal segment Ω_q and remove DC component;
4. Compute b and a according to Eq. 10 and Eq. 12;
5. If both changes in a and b are smaller than respective preset thresholds ϵ_b and ϵ_a , proceed to Step 6; otherwise go back to Step 4;
6. Check the change of the similarity measurement by Eq. 6. If it is larger than a preset threshold ϵ_s , go back to Step 2; otherwise stop.

In real situations, usually there is no model signal directly available. To estimate the model signal from a set of observed samples, we devise the following procedure: 1) Average all the signals in a pre-selected time segment and use the output (with DC removed) as the initial estimation of the model signal Ω_p ; 2) Use Ω_p and the above localization algorithm to find the transformed signal in each trial; 3) Compute the inverse-transformed observed signals and use their average as the new estimation for the model. Go to Step 2 until convergence on Ω_p occurs.

4. Evaluation with Computer Simulations

In this section we examine the proposed localization method in terms of robustness against additive noises. We use a segment of sinusoid as the model signal and transform it by $a = 1.65$ and $b = 14$. We have conducted a series of tests, with different levels of additive zero-mean Gaussian noises. Each test has 16 instances of transformed signals (with lead-in and lead-out segments for simulating pre and post motor imagination periods in real NIRS BCI trials). Fig. 2 gives an example where the noise level is $\sigma = 0.6$.

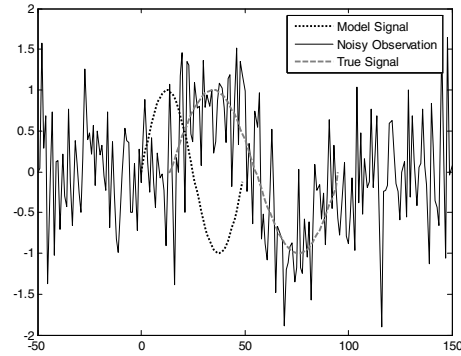


Figure 2. Simulation signals

The proposed method were applied to locate the transformed model signal in the random trials. The results in terms of means and deviations are plotted in Fig. 3.

The figure shows that the proposed method can accurately locate the signals even under severe noise corruptions (e.g. under $\sigma = 0.6$) plus considerable transformations.

5. Application to Motor-Imagery Classification

We developed a BCI system using a multi-channel NIRS instrument (OMM-1000 from Shimadzu Corporation, Japan) for measuring Oxy-Hb and Deoxy-Hb concentration

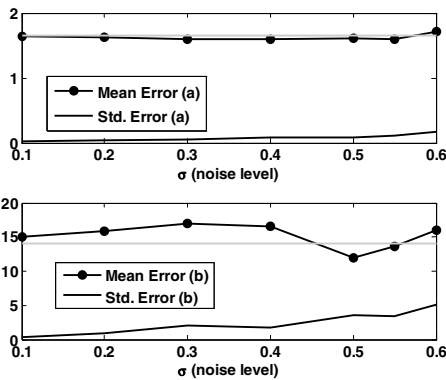


Figure 3. Results of Simulation

changes during a subject's mental activity. The sampling rate is 14Hz, and totally 20 channels are recorded to cover the main motor cortex. The Oxy-Hb and Deoxy-Hb signals are then processed to distinguish between two types of mental activities: imaginary left/right hand movements.

In order to evaluate the method in real situations, we have conducted a study that involves five healthy subjects, each subject performing 40/40 trials of left/right motor imagery tasks (see Fig. 1). We use the data during the imagination period (10 seconds) to do classification. The classification consists of three major steps of processing:

1. Preprocess by low-pass filtering (with cutoff frequency at 0.7Hz and stop frequency at 1.0Hz to remove artifacts from heart beat and high frequency noises);
2. Empirically select channels, and apply common spatial filtering [8] to stress discriminative information;
3. Find and recover the transformed signal in each trial using the proposed localization method;
4. Classify the signal with a support vector machine.

In the offline evaluation, we have run 8 rounds of 5-fold cross-validation on each subject, and compared the average accuracies with those by not using localization in Table 1.

6. Discussions

Table 1 shows that, the kernel localization can enhance the system performance in most cases while the accuracy on average turns considerably better (with 13.82% error reduction). It is thus suggested that the proposed method is effective and is useful for building high-performance BCI systems. It should also be mentioned that the proposed method

Subject	w/o localization	w/ localization	Err. Redu.
1	88.92 7.79	92.23 7.24	29.87%
2	64.04 10.11	63.74 9.55	-0.83%
3	66.63 11.90	74.60 9.87	23.88%
4	71.37 10.78	74.38 9.41	10.51%
5	63.49 10.28	65.56 9.54	5.67%
Average	70.89	74.10	13.82%

Table 1. Comparative Classification Accuracy for Motor Imagery.

may also be extended to other signals, e.g. functional MRI which detects the same physiological phenomenon, or surface EEG using event-related potentials such as P300.

References

- [1] J.R. Wolpaw, N. Birbaumer, D.J. MacFarland, G. Pfurtscheller, and T.M. Vaughan. Brain-computer interface for communication and control. *Clinical Neurophysiology*, 113:767–791, 2002.
- [2] J. Wolpaw and D. McFarland. Multichannel EEG-based brain-computer communication. *Electroencephalography. Clin. Neurophysiol.*, 90:444–449, 1994.
- [3] G. Pfurtscheller, C. Neuper, D. Flotzinger, and M. Prenger. EEG-based discrimination between imagination of right and left hand movement. *Electroencephalography. Clin. Neurophysiol.*, 8(4):441–446, 1997.
- [4] A. Villringer and H. Obrig. Near-infrared spectroscopy and imaging. In *Brain Mapping: The Methods*, pages 141–158. Elsevier Science (USA), 2002.
- [5] S. Coyle, T. Ward, C. Markham, and G. McDarby. On the suitability of near-infrared (nir) systems for next-generation brain-computer interfaces. *Physiological Measurements*, 25:815–822, 2004.
- [6] R. Sitaram, Y. Hoshi, and C. Guan. Near infrared spectroscopy based brain-computer interface. In *the Proc. of the International Conference on Experimental Mechanics*, 2004.
- [7] D. Scott. *Multivariate Density Estimation*. Wiley, New York, 1992.
- [8] Z.J. Kiles and A.C.K. Soong. EEG source localization: Implementing the spatio-temporal decomposition approach. *Electroencephalography. Clin. Neurophysiol.*, 107:343–352, 1998.